

Preferential Topography of Proteins Regulating Vascularization and Apoptosis in a MX1 Xenotransplant After Treatment With Hypoxia, Hyperthermia, Ifosfamide, and Irradiation

Oliver Schmitt, M.D., Christine Schubert, M.D., Thomas Feyerabend, M.D., Thomas Hellwig-Bürge, Ph.D., Christoph Weiss, M.D., and Wolfgang Kühnel, M.D.

The MX1 xenotransplant growing in nude mice was used as a model for estrogen- and progesterone-receptor-negative breast cancer. The effects of different therapeutic regimens—combinations of hyperthermia, chemotherapy, and irradiation—on the expression of proteins playing a role in tumor vascularization and apoptosis were investigated. Additionally, MX-1 tumors were exposed to hypoxia to investigate changes in protein expression related to angiogenesis. This is of particular importance with respect to antiangiogenic therapies that may be combined with the treatments mentioned before. Endothelial and adhesion factors, extracellular matrix (ECM) factors, apoptosis-regulating factors, and neuronal factors were examined by immunohistochemical techniques. Concerning vascularization, the most prominent changes were seen in the expression of vascular endothelial growth factor (VEGF) and basic fibroblast growth factor (bFGF), which increased strongly after hypoxia. The other cytokines, adhesion and ECM molecules, were either little affected or unaffected by the therapy. At the ultrastructural level, the walls of the tumor vessels are of the sinusoidal type, possessing many fenestrations. With regard to the second focus of this investigation, apoptosis, tumor cells again exerted the strongest differences after hypoxia where c-myc was clearly enhanced, whereas the effects on p53, bcl-2, and CD95 were extremely weak or not detectable. Furthermore, the neurotransmitter somatostatin, a possible “external” regulator of apoptosis, did not show treatment-related changes. In summary, it was shown that 1) within the group of apoptosis-regulating proteins c-myc was particularly affected by hypoxia, indicating a possible role for an activation-induced pathway of apoptosis in this context; 2) minor changes seen after treatment combined with hyperthermia point to a more acute vascular reaction (=dilatation), causing an increase of tissue pO_2 rather than angiogen-

esis; and 3) the concentrations of the angiogenic factors VEGF and bFGF rose strongly under hypoxia, thereby possibly exerting counterproductive effects to antiangiogenic therapy but not to thermochemotherapy or irradiation. This supports the concept of a combined antiangiogenic, hyperthermia, chemo- and irradiation therapy.

Key Words: Human breast carcinoma—Xenotransplant—Nu/nu mice—Hypoxia—Hyperthermia—Ifosfamide—Irradiation—Immunohistochemistry.

The results of several recent clinical studies indicate that the combination of chemotherapy and/or irradiation with hyperthermia improves therapeutic efficacy.¹⁻⁷ Concerning radiotherapy, it is well known that the efficacy of a given dose of irradiation depends to a large extent on the state of tumor oxygenation.⁸ Well-oxygenated tumors are more radiosensitive than poorly oxygenated tumors. Tissue oxygenation increases and decreases with blood supply. The latter, in turn, depends on the density of tissue vascularization and on the number of actually patent pathways. Hyperthermia at clinically used temperatures, i.e., 41°C to 43°C, elicits a rise of tissue pO_2 ^{9,10} caused by an increased blood flow in the tumor. Because increased vessel diameters were found in these tumors, vasodilation plays an important role in the increase of blood supply.¹¹

Thus, in the present study we investigated the effects of irradiation and/or ifosfamide combined with hyperthermia on the expression of proteins related to tumor vascularization with the aim of better understanding the role of these proteins in increasing the therapeutic efficacy of the previously mentioned combination therapies.

Previously it has been reported that irradiation,^{12,13} chemotherapy,¹⁴⁻¹⁷ hyperthermia,¹⁸ and hypoxia^{19,20} are involved in the regulation of apoptosis. Therefore, we studied the effects of physical and chemical treatments on MX1 tumor cells and their host tissue in nu/nu mice.

From the Departments of Anatomy (O.S., C.S., W.K.), Physiology (T.H.-B., C.W.), and Radiation Oncology and Nuclear Medicine (T.F.), Medical University of Lübeck, Lübeck, Germany.

This work is dedicated to our deceased friend and dear colleague PD Dr. med. Andrés S. Mendoza.

Address correspondence and reprint requests to Dr. O. Schmitt, Department of Anatomy, Medical University of Lübeck, Ratzeburger Allee 160, D-23538 Lübeck, Germany.

DOI: 10.1097/01.COC.0000017579.15196.14

TABLE 1. Survey of the different therapeutic regimens

Group	Abbreviation	Ifosfamide	Temperature	Irradiation	Hypoxia	Killing of animals
Control	—	—	RT	—	—	After tumor has reached 180 mm ³ in size
Ifosfamide	CT	✓	RT	—	—	1 or 2 h after treatment
Ifosfamide + irradiation + hyperthermia	XHT	✓	41°C	1 × 2 Gy	—	Directly after treatment
Ifosfamide + hyperthermia	TCT	✓	41.8°C	—	—	5 days after treatment
Irradiation + hyperthermia	XHT	—	41.8°C	1 × 2 Gy	—	Directly after treatment
Irradiation + hyperthermia	XHT	—	41.8°C	5 × 2 Gy	—	5 days after treatment
Ifosfamide + irradiation + hyperthermia	TCX	✓	41.8°C	1 × 2 Gy	—	Directly after treatment
Irradiation	XIR	—	RT	1 × 2 Gy	—	Directly after treatment
Irradiation	XIR	—	RT	5 × 2 Gy	—	Directly after treatment
Hypoxia	H3	—	RT	—	3 h	Directly after hypoxia
Hypoxia	H4	—	RT	—	6 h	Directly after hypoxia
Hypoxia	H5	—	RT	—	9 h	Directly after hypoxia
Hypoxia	H6	—	RT	—	17 h	Directly after hypoxia

MATERIALS AND METHODS

Xenotransplants of human breast cancer (MX1) were grown in thymus-aplastic nude mice (nu/nu).²¹ The MX1 tumor cell line was introduced as a model for human breast cancer by Wolpert-DeFilippes.²² The tumor is characterized as a solid, undifferentiated breast carcinoma with few necroses and no metastases (Tumorsteckbrief [IN-VIVO], Deutsches Krebsforschungszentrum, Heidelberg, Germany).

The tumors contain no significant concentrations of estrogen or progesterone hormone receptor proteins.²³

MX1 Tumor Cell Line and Xenotransplantation

A cell suspension of the MX1 culture (obtained from Deutsches Krebsforschungszentrum) was subcutaneously injected in the right hind paw of 6 to 8 weeks old female NMRI nu/nu mice (Zentralinstitut für Versuchstierzucht, Hannover, Germany). The animals received food and water ad libitum. After 3 weeks, tumor tissue of these inoculated mice (donor mice) was excised under sterile conditions and dissected into 1-mm³ cubes. These tumor cubes were transplanted in the right hind paw of recipient mice as described by Roszinski et al.¹⁰ and Wiedemann et al.^{23,24} Three to 4 weeks after the transplantation of the tumor cubes, the tumors had reached a mean volume of approximately 180 mm³.

Therapeutic Regimen

At this stage the tumor-bearing mice were treated as follows (Table 1): 1) the control group did not receive any treatment; 2) two groups were treated at room temperature with ifosfamide and the tumors were removed 1 hour and 2 hours after the end of treatment, respectively; 3) one group was treated with ifosfamide at 41.8°C, and the animals were killed 5 days later; 4) one group was treated with ifosfamide and 1 × 2 Gy at 41°C hyperthermia, and the animals were killed at the end of therapy; 5) another group was treated with ifosfamide and 1 × 2 Gy at 41.8°C, and the animals were killed after the end of therapy; 6) and 7) Two groups were treated with 1 × 2 Gy or 5 × 2 Gy, and subsequently the animals were killed; 8) one group was treated with 1 × 2 Gy and hyperthermia at 41.8°C, and subsequently the animals were killed; 9) one group was treated with 5 × 2 Gy and hyperthermia at 41.8°C, and the animals were killed 5 days after the end of therapy.

The immunohistochemical incubations were done in the

same way as those of the tissue samples of treated tumors. Only one control group was used because the treatment of the experimental groups was performed directly after killing the control group.

The objective of the group characterized at 2) was to find out if the vasculature is changing within a short delay after treatment. Additionally, it was unclear which and where certain proteins show differences in the expression. Under this aspect, groups 4), 5), and 8) were investigated also. A further aim was to study long-term effects under 5 × 2 Gy irradiation.

The aim of local hyperthermia in the clinical setting is to achieve a target temperature of 43°C. However, because of inhomogeneous perfusion of the tumor mass it has been impossible, so far, to attain 43°C in all parts of a tumor. Temperatures measured at randomly distributed loci in human tumors lay between 39°C and 45°C. The mean tumor temperatures were in the range between 41°C and 43°C.^{2,3} For our first series of experiments, we used 41°C. With the aim of increasing the efficacy of hyperthermia, we later raised the mean target temperature. At temperatures greater than 41.8°C, however, the tumors were destroyed and the effect of the different therapies could no longer be assessed. Furthermore, at temperatures greater than 41.8°C, only a few of the animals survived. Thus, we performed our second series of experiments at a target temperature of 41.8°C.

The animals were anesthetized with an intraperitoneal injection of 16 ml/kg body weight of 2 mg/ml pentobarbital (Nembutal: Sanofi Ceva, Hannover, Germany) and 1 mg/ml xylazine (Rompun: Bayer, Leverkusen, Germany) in 0.9% NaCl. Local hyperthermia was performed in a water bath heating only the right hind paw bearing the tumor. The temperatures of the water bath were adjusted according to the temperatures listed in Table 1. Hyperthermia in our setting was performed for 1 hour. Ifosfamide was injected intravenously into the tail vein at a concentration of 25 mg/ml in a dosage of 250 mg/kg body weight.

Ifosfamide is an oxazaphosphorine analogue of the well-established alkylating agent cyclophosphamide. Ifosfamide, like cyclophosphamide, is a prodrug that undergoes complex metabolism in vivo.^{25,26} The initial metabolism of ifosfamide consists of two different pathways. First, an enzymatic hydroxylation at carbon-4 forms 4-OH-ifosfamide, which is probably the major biologically active alkylating compound derived from ifosfamide, and second, a side-chain oxidation leads to the

TABLE 2. Overview of the antibodies used in this study

Protein family	Antigen	Manufacturer	Origin	Concentration
Extracellular matrix proteins	Fibronectin	Dako (A 245)	Rabbit	1:200
	Laminin	Sigma (L-9393)	Rabbit	1:100
	Collagen IV	Chemicon (AB756)	Rabbit	1:50
Vascular proteins	VWF	Sigma (F-3520)	Rabbit	1:500
	bFGF	Sigma (F-5337)	Rabbit	1:100
	Endothelin	Peninsula (MCE-6901-01)	Mouse FITC conj.	1:20
	PD-ECGF	Biermann (AB-229-NA)	Goat	1:100
	VEGF	Oncogene Science (PC 37)	Rabbit	1:20
Cell cycle regulatory proteins	Bcl-2	Santa Cruz (sc-492)	Rabbit	1:200
	C-myc	Biomol (06231)	Rabbit	1:500
	p53	Saxon (APNA05)	Rabbit	1:50
Adhesion proteins	CD34	Serotec (MCA547F)	Mouse FITC conj.	1:10
	CD31	Serotec (mca793f)	Mouse FITC conj.	1:10
	CD95	Immunotech (1506)	Mouse FITC conj.	1:500
Neuronal proteins	Somatostatin	Amersham (RPN 1612)	Rabbit	1:2,000
	NGF	Boehringer (1087754)	Mouse	1:200

bFGF, basic fibroblast growth factor; FITC, fluorescein isothiocyanate; NGF, neuronal growth factor; PD-ECGF, platelet-derived endothelial cell growth factor; VEGF, vascular endothelial growth factor; VWF, von Willebrand factor.

liberation of chloroacetaldehyde, a compound with possible neurotoxic properties.²⁷ Chloroacetaldehyde,²⁸ as well as hyperthermia,²⁹ causes glutathione depletion in vivo.

Hypoxia

Hypoxia was induced to mimic the hypoxic state occurring in areas of the tumor where O₂ consumption exceeds oxygen supply. Mice were put in a box of acrylic glass. The box was continuously ventilated by premixed gas (90% N₂, 10% O₂) under atmospheric pressure (normobaric hypoxia) for 1 hour, 3 hours, 6 hours, 9 hours, and 17 hours (Table 1).

Immunohistochemistry

For the subsequent histologic studies, the animals were perfused through the left ventricle with glucose Ringer solution containing sodium heparinate (1,000 IU/100 ml) and tissues were fixed with 4% neutral PBS (pH 7.4) buffered formalin solution. Thereafter, the tumors were removed and frozen in liquid nitrogen. Then 12- μ m-thick slabs were sectioned at -20°C on a cryostat and mounted onto chromalum gelatin prepared glass slides. After several rinsings in 0.1 mol/l PBS nonspecific binding of the sections was blocked for 30 minutes in 10% normal goat serum (Dako, \times 907).

Primary Antibodies From Rabbit

Sections were then incubated with the primary antibody raised against the different antigens as listed in Table 2 for 12 hours in a humid chamber at room temperature. Afterwards the antibody was rinsed off and the sections were washed for 10 minutes in PBS. As secondary antibody, the fluorescein isothiocyanate (FITC)-labeled goat antirabbit IgG (Dako, Z 421) was diluted 1:100 in PBS for 2 hours. Then sections were washed again and covered with glycerine PBS and coverslips for microscopic examination. For the production of stable stainings, the peroxidase technique was used. The coverslips were carefully removed and the sections were rinsed with PBS. They were incubated with goat anti-rabbit IgG for 12 hours in a humid chamber followed by washing with PBS. The specimens were then incubated for 3 hours in a solution containing a 1:100 diluted peroxidase-antiperoxidase complex (Dako, Z 113). Before a solution of PBS-diluted 4-chloro-1-naphthol or

diaminobenzidine (DAB) was used as the substrate for the peroxidase reaction, the specimens were washed again in PBS. The reaction was stopped by washing with PBS.

Control slides were rinsed with the buffer containing all ingredients except the primary antibody. After the reactions the slides were mounted with Aquatex (Merck, 8562).

Primary Antibody From Mice

Because mouse tissue is located in and around the xenograft, we used primary antibodies against endothelin, CD31 and CD34, which were directly conjugated to FITC. For immunoperoxidase staining, a goat antibody against FITC (Sigma F-2012) served as secondary antibody that was visualized with peroxidase-conjugated antibodies against goat IgG (Dako Z0421). Substrate reaction was performed as described herein.

For the neuronal growth factor (NGF) localization, NGF antibodies from mouse were labeled with FITC using 5(6)-carboxyfluorescein-*N*-hydroxysuccinimide ester (FLUOS). One milligram antibody was diluted in 1 ml PBS. Then 10 μ l FLUOS was added to 90 μ l dimethylsulfoxide. Sixteen microliters of this solution was added to the antibody-PBS mixture. The labeling was performed under gentle stirring in the dark. Two hours later, the nonreacted FLUOS was separated by a gel filtration or column chromatography using a Sephadex G-25 column, respectively. The last eluates contain the FITC labeled NGF antibodies, which were thereafter used for the staining as described herein.

Electron Microscopy

Only control tumors were fixed for transmission electron microscopy as follows: After washing out the blood with a glucose Ringer solution containing sodium heparinate (1,000 IU/100 ml) through the left ventricle in the anesthetized mice, for fixation of 2% glutaraldehyde and 0.6% paraformaldehyde in 0.06 mol/l sodium cacodylate buffer (pH 7.35) was used for perfusion, again, through the left ventricle. After 10 minutes of perfusion the tumors were excised and immersed in the same fixative for 72 hours at 4°C. The samples were then rinsed in 0.2 mol/l sodium cacodylate buffer and postfixed with 1% osmium tetroxide (OsO₄) in the same buffer, pH 7.35, for 2 hours at room temperature. After being rinsed in 2.4% NaCl,

the samples were washed in 0.2 mol/l sodium acetate buffer (pH 5.0) and block stained with 1% uranyl acetate in 0.2 mol/l sodium acetate buffer (pH 5.0) for 30 minutes in the dark and at room temperature. Routine procedures for dehydration in alcohol and embedding in araldite followed. Semithin sections (0.5 μm) were stained with azure II-methylene blue. Ultrathin sections (60 nm) were stained with lead citrate³⁰ and examined in a Philips 400 electron microscope.

Immunogold Electron Microscopy

The steps before the postfixation were the same as described for electron microscopy, but samples were rinsed in 0.1 mol/l sodium cacodylate and postfixation was performed in 2% aqueous OsO_4 solution for 2 hours followed by a further rinsing in 0.1 mol/l sodium cacodylate buffer. The sections were dehydrated in ascending 30% to 70% ethanol in 10% steps for 1 hour. Then they were first immersed in a 70% ethanol LR-white solution (1:1) for 1 hour followed by LR-white overnight at 4°C. The next day this was changed against fresh LR-white in which the samples were left for 3 days at 4°C. Subsequently, they were polymerized at 50°C for 36 hours. At first the sections were rinsed in three portions of Tris-buffered saline (TBS: 0.45 g NaCl + 0.605 g Tris(hydroxymethyl)-aminomethane + 100 ml aqua dest., adjusted to a pH of 7.4 with approximately 5 ml 1 N HCl) solution, and thereafter unspecific binding sites were blocked for 10 minutes with 0.5% bovine serum albumin solved in TBS. For the immunogold reaction, we used a primary polyclonal antibody raised in goat against human vascular endothelial growth factor (VEGF) (R&D AB-293-NA) at a concentration of 1:10 solved in a TBS with 0.01% Tween 20. The incubation lasted 12 hours and was performed at 22°C. Subsequently, the specimens were rinsed 5 times for 5 minutes in TBS. The incubation with the secondary antibody that was labeled before with 12 nm gold particles lasted 3 hours followed by a rinsing in TBS 4 times for 5 minutes. Finally, the antibody complexes were stabilized for 5 minutes in 2% glutaraldehyde solved in aqua dest. Specimens were rinsed again 2 times in aqua dest. and transferred to an ultrastainer (30 min uranyl acetate and 6 min lead citrate), which was performed as usual.³¹ The samples on the grids were examined with a Zeiss EM 109 at 60 kV.

RESULTS

The specific therapeutic effects of the different treatments are published by Wiedemann et al.^{4-7,23,24} and Feyerabend et al.^{2,3} In the following, the results of each protein or protein family are described. A graphical overview of all observations is given by Figure 1.

Immunoreactivity of Vascularization-Related Factors: Cytokines and Vasoactive Peptide

Aside from bFGF, VEGF or vascular permeability factor are the most potent and widely investigated angiogenic factors.³² VEGF acts as an endothelial cell mitogen in angiogenesis and neovascularization. Tumor growth depends on development of new capillaries and vessels. Therefore, the distribution of VEGF expression was investigated after the different therapeutic regimens. The MX1 tumors of the untreated, of the thermo-chemo-treated, and of the irradiated mice expressed no detectable amounts of VEGF. However, VEGF-immunoreac-

tive cells were observed in hypoxic mice (10% O_2 : 1 hour, 3 hours, 6 hours, 9 hours, and 17 hours). VEGF was found in the cytoplasm of the tumor cells and in fibroblasts (Fig. 2a and b), and was less pronounced in endothelial cells in the connective tissue (Fig. 2c and d). A clear upregulation of VEGF immunoreactivity was observed in mice exposed for 9 and 17 hours to hypoxia (Fig. 2a). VEGF expression increased with the duration of the exposure to hypoxia. The immunogold method confirmed the light microscopy findings. In Figure 3b, gold particles are clearly visible within the cytoplasm of an MX1 tumor cell.

The vasoactive peptides endothelin ET-1 and ET-3 stimulate the synthesis of VEGF³³ and were, therefore, of great interest in this context also. Figure 4c demonstrates that ET-1 is expressed by MX1 cells of the control group, but a stronger staining was detected in the peritumoral wall of connective tissue.

Basic fibroblast growth factor (bFGF or FGF-2) belongs to the family of fibroblast growth factors (FGF-1 to FGF-9), which are polypeptides that are potent regulators of cell proliferation, differentiation, and function.³⁴ Together with acidic FGF, it is also chemotactic and mitogenic for endothelial cells in vitro. It induces the endothelial cell production of enzymes involved in breakdown of basement membranes and the migration of endothelial cells in collagen matrices to form capillary-like tubes.³⁵⁻³⁷

In our experimental setup, bFGF was expressed in MX1 tumors of the control group and in all hypoxic groups (Fig. 5a and b) with the highest level of immunoreactivity in hypoxic tumor tissue. This observation is in agreement with the findings of Le and Corry³⁸ as well as Koong et al.³⁹ However, we could not detect bFGF immunoreactivity in the tumors treated by thermochemotherapy and irradiation.

Platelet-derived endothelial cell growth factor (PD-ECGF) was originally isolated from platelets as a protein with specific mitogenic activity for endothelial cells.⁴⁰ PD-ECGF is reportedly produced by several types of tumor cells also.⁴¹ It has been shown to induce angiogenesis in the chick chorioallantoic membrane as reported by Ishikawa et al.⁴² In our experiments, little immunoreactivity was seen in the tumors treated by thermochemotherapy and by irradiation. There was no PD-ECGF immunoreactivity observed in hypoxic tumors.

Cell Adhesion Molecules

The cell adhesion molecules CD31 (PECAM) and CD34, which served as endothelial cell markers,⁴³⁻⁴⁷ are located at the luminal side as an endothelial-cell-specific surface antigen. However, Hettasch et al.⁴⁴ showed that tumor cells at the boundary to normal tissue can express CD31, CD34, and von Willebrand factor (VWF). In general, the expression of CD31 and CD34 was more obvious in tumors of the control group than in tumors treated by thermochemotherapy or irradiation (Fig. 4a and b).

CD31 was found around the cytoplasm in close proximity to the cytomembrane of endothelial cells and of a

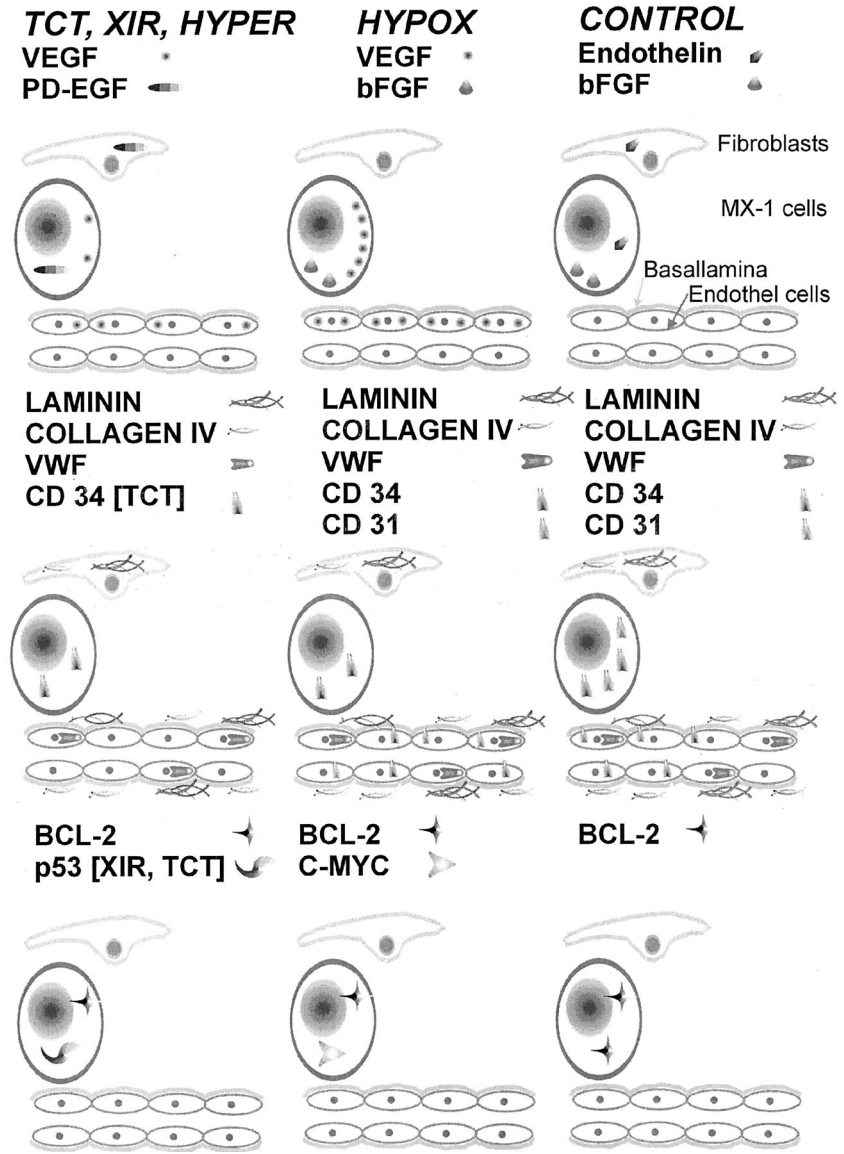


FIG. 1. Overview of results. The left column shows the results in TCT, XIR and hyperthermia (HYPER) treated tumor tissue. The column in the middle represents the findings in the hypoxia experiments. The right column gives an overview of the histologic observations made in the untreated tumors. The first row shows the angiogenesis-associated protein expressions. The middle row shows the distribution of the vascular associated proteins and the extracellular matrix proteins laminin and collagen IV. The last row documents the observations of some cell cycle- and apoptosis-associated proteins.

few tumor cells in MX1 control and all hypoxic groups (Fig. 4a). The irradiated tumors and the tumors treated by thermochemotherapy showed no immunoreactivity for CD31. CD34 was detected in the area of the cytomembrane of tumor cells of the control group and after thermochemotherapy but not after irradiation (Fig. 4b). Additionally, it was expressed in all hypoxic tumors. CD34 was found mainly in the cytoplasm of tumor cells, especially in hypoxic tumors. However, the immunoreactivity observed in the tumor cells of the hypoxic group was weaker than at the membranes of tumor cells after thermochemotherapy and in untreated tumors (Fig. 6b).

Factor VIII-Associated Antigen (Endothelial Cell Marker)

The VWF or factor VIII antibodies bind to VWF mainly located in the Weibel-Palade bodies in endothe-

lial cells and, therefore, serve as an additional marker for these cells. The VWF protein was depictable in all tumors independent of the treatment regimen. We have observed that, at the border region between MX1 tumor cells and host tissue, immunoreactivity for VWF was stronger than inside the tumor (Fig. 4d).

Immunoreactivity of Extracellular Matrix Molecules

Tumors often show irregularities regarding the organization of the extracellular matrix (ECM), especially at their basement membrane.⁴⁸ This may indirectly be induced by bFGF, which stimulates the production of matrix metalloproteinases.⁴⁹⁻⁵¹ After the rise of bFGF was detected, it seemed expedient to investigate ECM molecules for structural changes. However, in our experiments the ECM proteins collagen IV (Fig. 7b), fibronec-

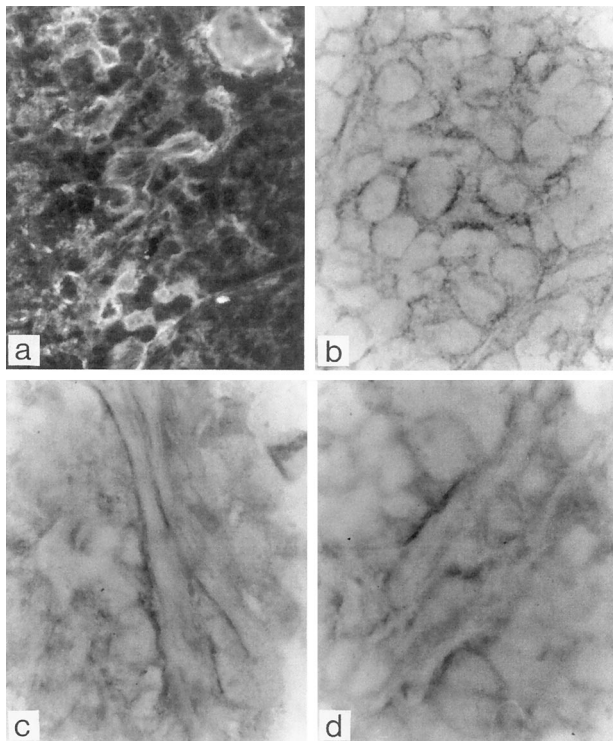


FIG. 2. Vascular endothelial growth factor (VEGF) expression in a MX1 tumor of nu/nu mice exposed 3 hours to 10% O₂. **a.** The immunoreactive regions are located in the cytoplasm of MX1 cells (fluorescence, $\times 600$). **b.** Close to the cytomembrane (bright field, $\times 1,000$). In **(c)** and **(d)** endothelial cells of the vascular wall show immunoreactivity for VEGF (bright field, $\times 1,000$).

tin (Fig. 7c), and laminin (Fig. 7c) were found in the typical location in all MX1 tumors regardless of the treatment strategy (Fig. 7a–e). Because laminin and collagen IV are constitutional elements of the basal lamina, the vascular bed can indirectly be recognized by staining with the corresponding antibodies (Fig. 7a and b). The photomicrographs show the typical lobulation of the tumor by connective tissue. Between the MX1 cell agglomerates the connective tissue carries many larger vessels and capillaries (Fig. 7d and e). At the border between the tumor and the host tissue the connective tissue is stronger than in the septa which originate from the tumor capsule (Fig. 7a and b).

Immunoreactivity of Proteins Related to Apoptosis

The p53 gene is the most commonly mutated gene in human cancer and is an important regulator of apoptosis. It downregulates bcl-2 expression and upregulates bax expression, but may not always be necessary for apoptosis.^{52,53} A low p53 expression was found in the cytoplasm of individual tumor cells in hyperthermia-treated and irradiated (41.8°C + 5 \times 2 Gy) xenotransplants only (Fig. 8a).

The members of the Bcl-2 family of proteins interact

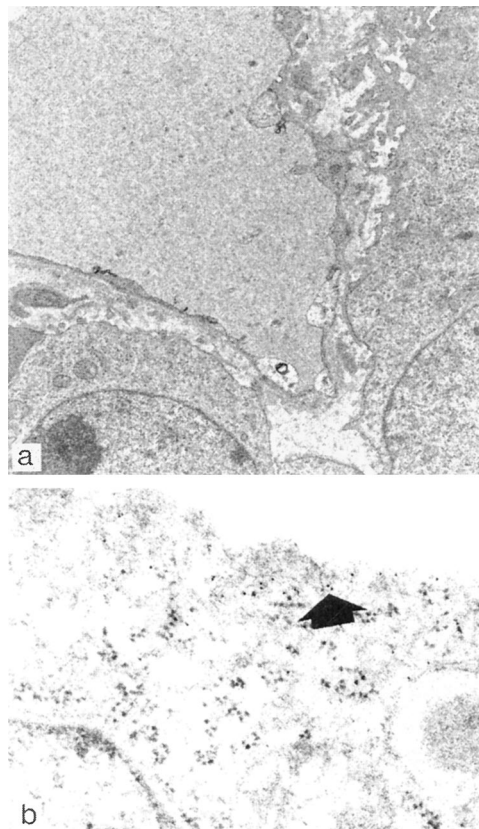


FIG. 3. **a.** The depicted part of a vessel shows fenestrations and an overlap of endothelial cell processes ($\times 6,000$). **b.** This image presents part of a MX1 tumor cell. The immunogold reactivity for vascular endothelial growth factor is visible (arrow) within the cytoplasm of the tumor cell.

to regulate programmed cell death, or apoptosis. Bcl-2 blocks programmed cell death by binding bax after a variety of stimuli.⁵⁴ Bcl-2 was clearly expressed in the cytoplasm of all MX1 tumor cells (Fig. 8d), regardless of the treatment.

C-myc is one of the three prototype members of the Myc gene family (c-myc, N-myc, L-myc) that belongs to the group of regulatory transcription factors. Expression of myc may be necessary for activation-induced cell death.⁵⁵ Therefore, deregulated c-myc expression is a potent inducer of apoptosis. In this study, only a few tumor cells from hypoxic xenotransplants (10% O₂: 3 hours) showed immunopositive c-myc sites (Fig. 8b). Proliferating cell nuclear antigen and Ki-67 expression was found only in a few MX1 cells (Fig. 8c and 8e).

CD95 (=FAS =APO-1), a member of the tumor necrosis factor receptor superfamily, is a cell surface receptor that induces apoptosis. Keane et al.⁵⁶ have shown that as opposed to breast cancer cells, normal breast epithelial cells express high levels of Fas mRNA. Only in the relatively benign breast cancer cell line T47D apoptosis can be induced by Fas activation.⁵⁶ The MX1

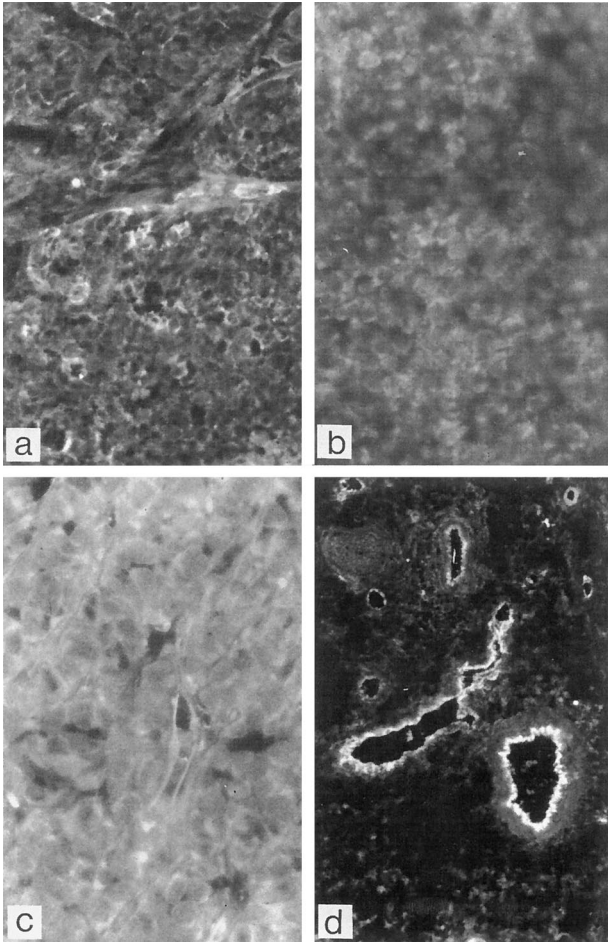


FIG. 4. Fluorescence photomicrographs of vessel-associated markers. **a.** CD31 immunoreactive MX1 tumor cells and an immunopositive vascular wall ($\times 400$). The adhesion molecules are localized in the cytoplasm of MX1 tumor cells. **b.** CD34 expression in the cytoplasm of MX1 cells ($\times 600$). **c.** Endothelin localization in a hypoxic MX1 tumor (3 hours 10% O_2). **d.** This photomicrograph documents the distribution of von Willebrand factor in the vascular wall (endothelial side) of larger vessels ($\times 100$).

cells used for this study did not express CD95, and none of the therapeutic regimens was able to induce it.

Neuronal Immunoreactivity

NGF—as a marker for neurons—and the neurotransmitter somatostatin were examined because of ultrastructural findings of nerve fibers (Fig. 6a). Somatostatin and its analogues (BIM23014, SMS 201–995) were of particular interest for this study because it was reported that somatostatin exerts direct antineoplastic effects with cytostatic (growth arrest) or cytotoxic (apoptosis) consequences.⁵⁷

NGF staining confirmed the existence of nerve fibers in the periphery of the tumor mass (Fig. 6c). In this study, we especially looked for immunoreactive sites of

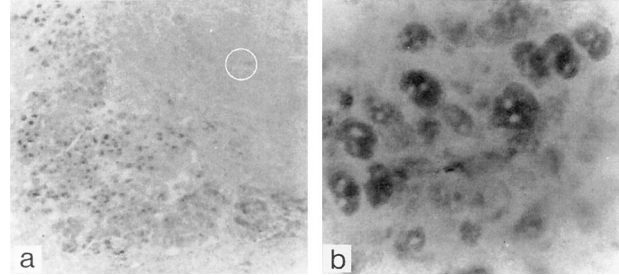


FIG. 5. **a.** Overview of bFGF positive MX1 tumor cells ($100\times$). In necrotic tumor mass no immunoreactivity for basic fibroblast growth factor (bFGF) (circle) is seen. **b.** The distribution of bFGF can be observed within the cytoplasm of MX1 cells only ($\times 1,000$). The nuclear regions (pale dots) are immunonegative.

nontumor cells to see whether these cells would be stimulated to produce somatostatin and could thereby contribute to the inhibitory effects of the treatment. However, very little somatostatin reactivity was detected within the connective tissue (Fig. 6b) of control tumors and only sporadic staining was found in tumors after thermochemotherapy. Thus, a regulative function from the host tissue via somatostatin seems unlikely.

Ultrastructure of Vessels

The ultrastructural morphology of the vascular wall showed frequently sinus-like vessels with fenestrations (Fig. 9a–b and Fig. 3a). These were often observed within the vascular bed of the tumor. Beside these typical fenestrations, overlapping of endothelial cytoplasm fenestration was observed (Figs. 3a, 9b). Thus far, fenestrations in capillaries within the tumor masses of hepatoblastoma^{58,59} and brain tumors^{60,61} were reported but not in MX1 tumors or other malignant tumors of the breast.

DISCUSSION

The ultrastructural and light microscopic morphology of MX1 xenotransplants—the model used in this study—was studied by Mendoza et al.⁶² Fundamental stereologic analysis of the tumor cell nuclei with respect to early changes after certain treatment strategies have been made by Krüger⁶³ and histochemical changes were reported by Stobbe.⁶⁴ Alterations of cell nuclei and nucleolar organizer regions were published by Schmitt et al.⁶⁵ Physiologic and metabolic data, i.e., pH, pO_2 and the activated form of ifosfamide (4-hydroxyifosfamide) of the MX1 xenotransplant under chemotherapy with ifosfamide at different temperatures were reported by Wiedemann et al.²⁴ and Mentzel et al.⁶⁶

Based on the data obtained in these reports, we aimed to further study mechanisms a) of the inhibitory effects of chemotherapy and/or irradiation combined with hyperthermia; and b) of hypoxic effects on the expression of angiogenic factors in situ. Hyperthermia and hypoxia influence tissue pO_2 and are thus factors determining cell

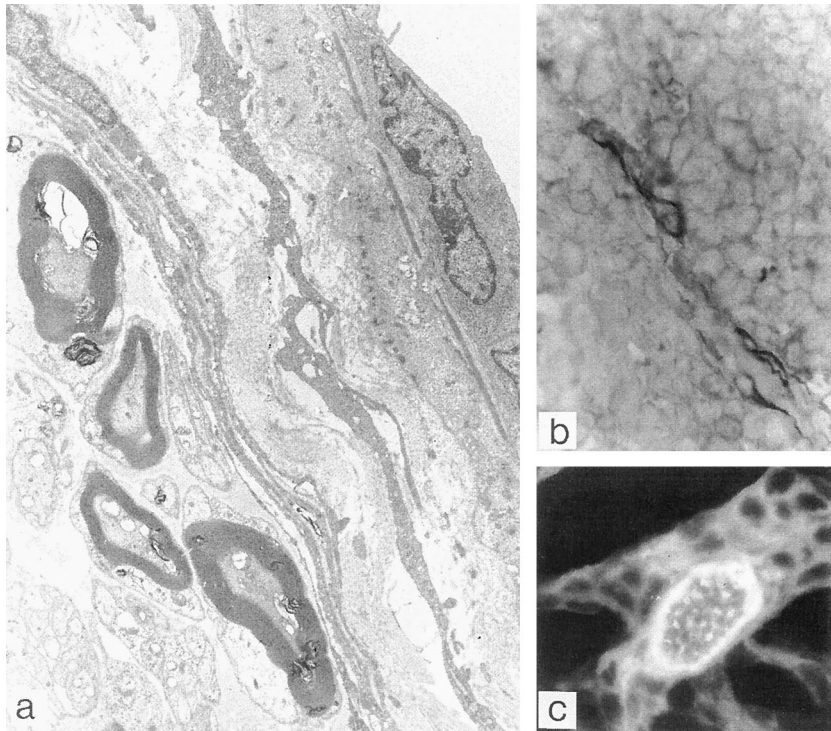


FIG. 6. **a.** In this electron microscopy image of an MX1 tumor, nerve fibers can be seen. This region was located in the MX1 tumor ($\times 6,000$). **b.** In some septa in between the tumor masses, somatostatin-positive regions were observed. **c.** Immunoreactive nerve fiber expressing nerve growth factor (fluorescein isothiocyanate immunofluorescence, $\times 1,000$).

proliferation or death.^{23,67} However, the exact mechanisms of their actions are still unclear. The results of Wiedemann et al.,²³ and of Murell⁶⁷ and quantitative studies on the angioarchitecture by Schmitt et al.¹¹ strongly suggest that tumor vasculature may play an important role in establishing the increased inhibitory effects after hyperthermia. The present article focuses on vascularization and related factors such as VEGF and on cell death.

VEGF and bFGF are most potent angiogenic factors, e.g., inducing endothelial mitosis, thus playing an important role in angiogenesis,³² which in turn is a prerequisite for tumor growth. In our experimental setup we found changes in VEGF expression only after hypoxia. This observation is in accord with results from Marxsen et al.,⁶⁸ who detected a strong increase in VEGF-mRNA in tumors of MX1-xenotransplanted nu/nu mice after 9 and 17 hours of hypoxia (10% O₂ in the inspiration atmosphere). The deficiency in oxygen seemed to mainly induce VEGF production in tumor cells and in fibroblasts—a mechanism by which the tumor could stimulate angiogenesis and, thus, upregulate its own blood supply as also suggested by Harmey et al.,⁶⁹ Harris et al.,⁷⁰ and Petit et al.⁷¹ Hyperthermia, however, did not influence VEGF immunoreactivity, probably because the increase of mean tissue pO₂ reduces the stimulus for the production of VEGF.

A physiologic stimulator, ET-1, of VEGF synthesis was not influenced by any of the therapeutic regimens. Thus, ET-1 can be ruled out as a factor inducing angiogenesis, indicating that other mechanisms cause the increase of VEGF production. The other very potent angiogenic cytokine besides VEGF is bFGF (FGF-2). Like

VEGF it provides mitogenic and chemotactic signals and serves as an important regulator of cell proliferation, differentiation, and cell function not only for fibroblasts but also for endothelial cells.⁷² Additionally, bFGF is of particular importance for the breakdown of ECM during endothelial migration. Data from *in vitro* experiments show that bFGF stimulates endothelial cells to produce proteinases that digest their basement membrane, to migrate and to form new capillary-like tubes.^{35–37} Furthermore, bFGF induces mitosis and the migration of endothelial cells.

This leads to the formation of new vessels.⁷³ Our results indicate that bFGF, like VEGF production, rises in hypoxic groups but remains unchanged after the other treatment strategies. Both factors seemed to be responsible for inducing angiogenesis in tumors that become O₂ deficient—a scenario occurring not only after inhibition of angiogenesis but also during phases of rapid tumor growth. In situations like that, tumor cell proliferation in relation to nutrient supply is too high and cells start dying. To save the tumor from complete regression, cells may produce angiogenic factors like VEGF and bFGF to upregulate blood supply and increase the tissue pO₂. For antiangiogenic therapy (depending on the strategy), it might, therefore, be crucial to additionally block VEGF and bFGF action.⁷¹ The third, less potent angiogenic cytokine, PD-ECGF, studied here has also been shown to be synthesized by several types of tumor cells.^{41,42} However, in our studies, overall expression of the factor was too weak to reveal changes. Although PD-ECGF cannot completely be ruled out,⁷⁴ yet the massive changes of VEGF and bFGF speak in favor of a more important role

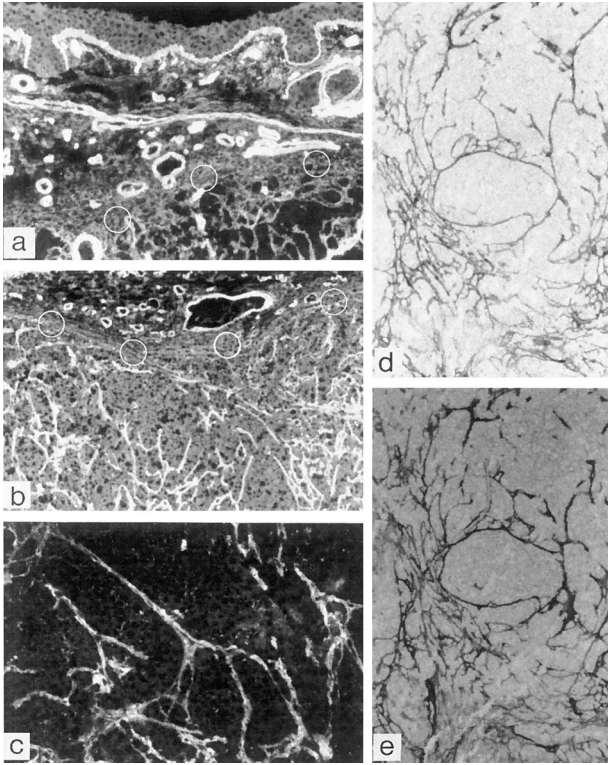


FIG. 7. Extracellular matrix. Overview of the laminin (fluorescence, $\times 100$) (a) and (b) collagen IV (fluorescence, $\times 100$). The border to the tumor tissue is indicated by circles. The connective tissue that constitutes the capsule of the tumor is clearly visible in (b). The walls of vessels show a characteristic fluorescence. c. Fibronectin shows the same distribution and appearance as laminin and collagen IV (fluorescence, $\times 1,000$). d. Collagen IV and in a consecutive section (e) laminin immunoreactive sites (bright field, $\times 600$).

for these cytokines in the hypoxic situation. The lack of changes in VEGF and bFGF under hyperthermia, however, together with the stereologic data on the early capillary changes and late vascular reactions indicating an increase of the average capillary diameter,¹¹ strongly point to an acute vascular reaction that enhances tissue pO_2 . Thus, it seems unlikely that the relatively slow process of angiogenesis is responsible for the observed swift rise of O_2 supply, because high VEGF and bFGF levels could have counteracted the effects of antiangiogenic therapy. This further supports the idea that a combined treatment (TCT, irradiation, and antiangiogenesis) would be advantageous for the patients.

The pattern of expression of CD31 and CD34 is comparable to the immunoreactivity of VWF. At the border of the tumor cell mass to the host tissue, CD31 and CD34 could be observed in higher concentrations than inside the tumor. This finding is in keeping with the observation that the peritumoral vessel density is larger than that inside the tumor. The lower expression of CD31 and CD34 in the tumor could be interpreted as a dys-

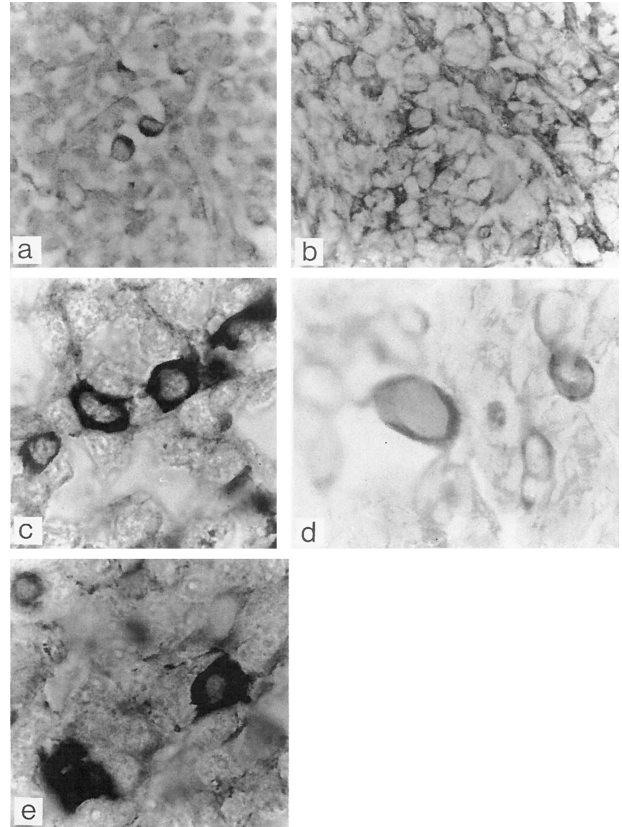


FIG. 8. This series of photomicrographs shows proteins that are associated with cell cycle- and apoptosis-associated proteins. a. p53 expression in the cytoplasm of a few tumor cells that were treated by TCT (DAB reaction, $\times 600$). b. C-myc is expressed in the cytoplasm of a few hypoxic MX 1 tumor cells (3 hours 10% O_2) (4-chloronaphthol reaction: 4CN, $\times 600$). c. Some tumor cells express proliferating cell nuclear antigen and (e) KI-67 (4CN reaction, $\times 1,000$). d. Bcl-2 is localized in the cytoplasm of MX1 tumor cells (DAB reaction, $\times 1,200$).

regulation in parts of the tumor showing high rates of mitosis with insufficient primary vascularization and an inadequate neovascularization that, as mentioned before, becomes too low with regard to tumor growth. Antiangiogenic therapy may, therefore, be effective by suppressing angiogenesis in the peritumoral border region rather than through effects on the tumor cells.

The expression of VWF, another endothelial cell marker, was not constant, which may be because of sporadic formation of Weibel-Palade bodies. The typical distribution with enhanced VWF immunoreactivity toward the host tissue could be interpreted as a sign for high mitotic activity in endothelial cells, which in turn do not differentiate enough to build these bodies.

Besides these light microscopic studies, the vascularization of xenotransplants was also studied by transmission electron microscopy. At the ultrastructural level, the sinusoidal walls displayed many fenestrations (Fig. 9a-b), a result that is consistent with findings of Roberts and

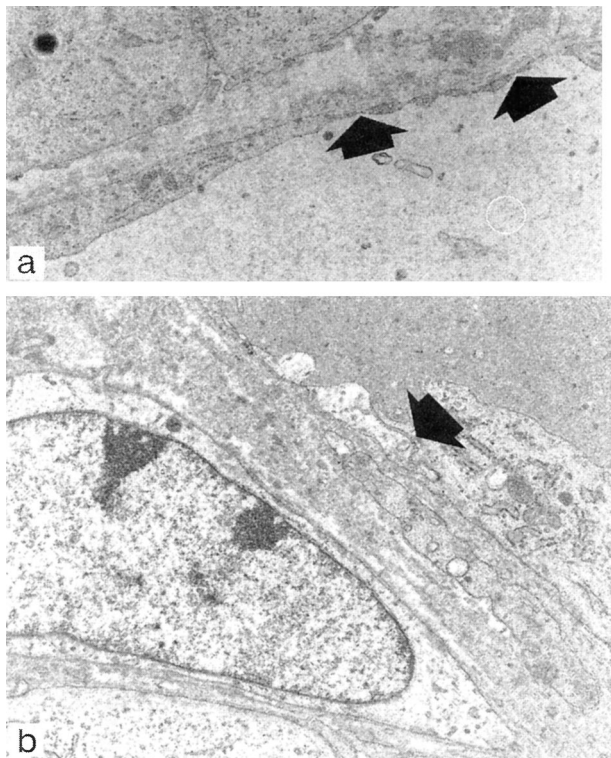


FIG. 9. Transmission microscopy photomicrographs of the vascular wall in control tumors ($\times 6,000$). **a.** The lumen of the vessels is indicated by a circle. The fenestrations are indicated by arrows. In **(b)**, an overlapping of endothelial cell processes is also indicated by an arrow.

Pallade⁷⁵ and Esser et al.⁷⁶ These openings are of particular interest insofar as they could act as gates for large molecules allowing anticancer therapeutics, e.g., antibodies easier access to the tumor cells. Further studies on the mechanisms of fenestration development with different methods, such as intravenous injections of cationic ferritin, are in progress.

As already mentioned, changes in ECM—especially in basement membrane—are often associated with tumor progression⁴⁸ and are also necessary for angiogenesis. Because of the stimulation of fibroblasts^{77,78} laminin, collagen IV, and fibronectin, which are also important components of the basement membrane of surrounding endothelial vessel cells were examined. There were no immunohistochemical differences between treated groups and the control groups, although bFGF was clearly upregulated in hypoxic tumors. However, one has to bear in mind that the samples could have been taken too soon after the rise in bFGF or that fragments of matrix molecules still contained the complete epitopes recognized by the antibodies. At this point, further investigations, for example, of metalloproteinases, will be necessary for a better understanding of the interactions between tumor cells and ECM in this experimental setup.

In the second part of our study, we investigated proteins related to apoptosis because through regulating

tissue pO_2 or via other mechanisms, hyperthermia as well as hypoxia may influence cell survival and death. Reports on induction of programmed cell death by hyperthermia^{79–81} and hypoxia⁸² suggest that both mechanisms induce apoptosis. We examined p53, bcl-2, c-myc, and CD95 (Fas).

The p53 gene is the most commonly mutated gene in human cancer and belongs to the group of proteins that induce apoptosis. It downregulates bcl-2 and upregulates bax expression, but may not always be necessary for apoptosis.^{52,53} Bcl-2, however, belongs to the group of survival genes and is able to prevent apoptosis induced by p53.⁸³ CD95 (=FAS =APO-1) is a cell surface receptor that triggers apoptosis⁵⁶ whereby part of the underlying mechanism is independent of bcl-2.⁸⁴ C-myc may be important for activation-induced cell death.⁵⁵ Therefore, deregulated c-myc expression could be a potent inducer of apoptosis also.

Bcl-2 and c-myc could be detected in the cytoplasm of all tumor cells, but although c-myc expression was most prominent in hypoxic groups, we did not see any treatment-related changes in bcl-2. These results indicate that c-myc could be part of the mechanisms inducing apoptosis after hypoxia as also suggested by Yao et al.,⁸² whereas bcl-2 may either not influence cell death at all in this setup or could indirectly be regulated through changes in the amounts of bax.⁸⁵ The appearance of low p53 levels in individual MX1 cells after thermochemotherapy could be interpreted as a “side effect” in the sense that some cells are more responsive to physical and chemical stress than others and undergo apoptosis.

The investigation of NGF and somatostatin was motivated by ultrastructural findings in nerve fibers, where the neurotransmitter somatostatin and its analogues (BIM23014, SMS 201–995) have been shown to exert direct antineoplastic effects with cytostatic (growth arrest) or cytotoxic (apoptosis) consequences.⁸⁶ This effect could be part of the mechanisms inhibiting tumor growth after the different therapeutic regimen suggesting an “external” regulator for tumor growth. The nerve fibers found in the MX1 xenotransplants should belong to the host’s peripheral nervous system, and the tumor could have either developed around them without any functional interaction or may have “recruited” them for the innervation of its own vasculature. However, somatostatin levels seemed to be very low throughout all experiments. Thus, at least for the times after the samples were taken, a regulative function of neurons for tumor cells via somatostatin seems unlikely.

In this study we analyzed xenotransplanted MX1 tumors for factors related to tumor vascularization and apoptosis after different therapeutic regimens.

It was shown that 1) within the group of apoptosis-regulating proteins, c-myc was particularly affected, indicating an important role for an “activation-induced” pathway of apoptosis after hypoxia; 2) the minor changes seen after treatments combined with hyperthermia point to an acute vascular reaction (=dilatation) causing an increase in pO_2 rather than any kind of angiogenesis; and

3) the angiogenic factors VEGF and bFGF rose strongly under hypoxia, thus possibly counteracting antiangiogenic therapy but not inhibiting the effects of irradiation or thermochemotherapy.

The latter are the most interesting results of the study showing that there is no uniform reaction pattern of allied members of the protein families studied here. This may indicate that specific inhibitors for certain angiogenic factors might be advantageous for antiangiogenic treatment. Combinations of inhibitors of angiogenesis and irradiation and/or thermochemotherapy may exert synergistic antitumoral effects. 

REFERENCES

1. Brizel DM, Scully SP, Harrelson JM, et al. Radiation therapy and hyperthermia improve the oxygenation of human soft tissue sarcomas. *Cancer Res* 1996;56:5347-50.
2. Feyerabend T, Steeves R, Wiedemann GJ, et al. Local hyperthermia, radiation, and chemotherapy in locally advanced malignancies. *Oncology* 1996;53:214-20.
3. Feyerabend T, Steeves R, Jäger B, et al. Local hyperthermia, hyperfractionated radiation, and cisplatin in preirradiated recurrent lymph node metastases of recurrent head and neck cancer. *Int J Oncol* 1997;10:591-5.
4. Wiedemann GJ, d'Oleire F, Eleftheriadis S, et al. Ifosfamide and carboplatin combined with 41.8°C whole-body hyperthermia in patients with refractory sarcoma and malignant teratoma. *Cancer Res* 1994;54:5346-50.
5. Wiedemann GJ, Robins HI, Gutsche S, et al. Ifosfamide, carboplatin and etoposide (ICE) combined with 41.8°C whole body hyperthermia in patients with refractory sarcoma: a phase II study. *Eur J Cancer* 1996;32A:888-92.
6. Wiedemann GJ, Robins HI, Katschinski DM, et al. Klinische Studien zur Kombination von Ifosfamid, Carboplatin und Etoposid (ICE) mit 41.8°C Ganzkörperhyperthermie. *Med Klin* 1996;91:279-83.
7. Wiedemann GJ, Robins HI, Katschinski DM, et al. Systematic hyperthermia and ICE chemotherapy for sarcoma patients: rationale and clinical status. *Anticancer Res* 1997;17:2899-902.
8. Tubiana M, Dutreix J. *Introduction to radiobiology*. London: Taylor & Francis, 1990.
9. Overgaard J, Overgaard M. Hyperthermia as an adjuvant to radiotherapy in the treatment of malignant melanoma. *Int J Hyperthermia* 1987;6:483-501.
10. Roszinski S, Wiedemann G, Jiang SZ, et al. Effects of hyperthermia and/or hyperglycemia on pH and pO₂ in well oxygenated xenotransplanted human sarcoma. *Int J Radiat Oncol Biol Phys* 1991;20:1273-80.
11. Schmitt O, Eggers R, Mendoza A, et al. Stereologic evaluation of the vasculature in a MX1 xenotransplanted tumour model after combinations of treatment with ifosfamide, hyperthermia and irradiation. *Int J Hyperthermia* 1999;15:237-50.
12. Meyn RE, Stephens LC, Mason KA, et al. Radiation-induced apoptosis in normal and pre-neoplastic mammary glands in vivo: significance of gland differentiation and p53 status. *Int J Cancer*, 1996;65:466-72.
13. Paglin S, Delohery T, Erlandson R, et al. Radiation-induced micronuclei formation in human breast cancer cells: dependence on serum and cell cycle distribution. *Biochem Biophys Res Commun* 1997;237:678-84.
14. Muller M, Wilder S, Bannasch D, et al. p53 activates the CD95 (APO-1/Fas) gene in response to DNA damage by anticancer drugs. *J Exp Med* 1998;188:2033-45.
15. Schwartz GK, Farsi K, Maslak P, et al. Potentiation of apoptosis by flavopiridol in mitomycin-C-treated gastric and breast cancer cells. *Clin Cancer Res* 1997;3:1467-72.
16. Giannios J, Ioannidou-Mouzaka L. Molecular aspects of breast and ovarian cancer. *Eur J Gynaecol Oncol* 1997;18:387-93.

17. Wagener C, Bargou RC, Daniel PT, et al. Induction of the death-promoting gene bax-alpha sensitizes cultured breast-cancer cells to drug-induced apoptosis. *Int J Cancer* 1996;67:138-41.
18. Toyota N, Strelbel FR, Stephens LC, et al. Long-duration, mild whole body hyperthermia with cisplatin: tumour response and kinetics of apoptosis and necrosis in a metastatic rat mammary adenocarcinoma. *Int J Hyperthermia* 1997;13:497-506.
19. Koester SK, Schlossman SF, Zhang C, et al. APO2.7 defines a shared apoptotic-necrotic pathway in a breast tumor hypoxia model. *Cytometry* 1998;33:324-32.
20. Amirkhosravi A, Meyer T, Warnes G, et al. Pentoxifylline inhibits hypoxia-induced upregulation of tumor cell tissue factor and vascular endothelial growth factor. *Thromb Haemost* 1998;80:598-602.
21. Pantelouris EM, Hair J. Thymus dysgenesis in nude (nu nu) mice. *J Embryol Exp Morphol* 1970;24:615-23.
22. Wolpert-DeFilippes MK. Antitumor activity of cis-dichlorodiammineplatinum(II). *Cancer Treat Rep* 1979;63:1453-8.
23. Wiedemann G, Roszinski S, Biersack A, et al. Treatment efficacy, intratumoral pO₂ and pH during thermochemotherapy in xenotransplanted human tumors growing in nude mice. *Contrib Oncol* 1992;42:556-65.
24. Wiedemann GJ, Siemens HJ, Mentzel M, et al. Effects of temperature on the therapeutic efficacy and pharmacokinetics of ifosfamide. *Cancer Res* 1993;53:4268-72.
25. Kurowski V, Cerny T, Küpfer A, et al. Metabolism and pharmacokinetics of oral and intravenous ifosfamide. *J Cancer Res Oncol* 1991;117:148-53.
26. Wagner T, Peter C, Voelcker G, et al. Characterization and quantitative estimation of activated cyclophosphamide in blood and urine. *Cancer Res* 1977;37:2592-6.
27. Goren MP, Wright RK, Pratt CB, et al. Dechloroethylation of ifosfamide and neurotoxicity. *Lancet* 1986;2:1219-20.
28. Lind MJ, McGown AT, Hadfield JA, et al. The effect of ifosfamide and its metabolites on intracellular glutathione levels in vitro and in vivo. *Biochem Pharmacol* 1989;38:1835-40.
29. Hahn GM. *Hyperthermia and cancer*. New York: Plenum Publishing, 1982.
30. Reynolds ES. The use of lead citrate at high pH as an electron-opaque stain in electron microscopy. *J Cell Biol* 1963;17:208-12.
31. Klinger M, Klüter H. Immunocytochemical colocalization of adhesive proteins with clathrin in human blood platelets: further evidence for coated vesicle-mediated transport of von Willebrand factor, fibrinogen and fibronectin. *Cell Tissue Res* 1995;279:453-7.
32. Folkman J. Tumor angiogenesis. In: Medelsohn J, Howley PM, Israel MA, et al., eds. *The molecular basis of cancer*. Philadelphia: WB Saunders, 1995:206-32.
33. Matsuura A, Yamochi W, Hirata K, et al. Stimulatory interaction between vascular endothelial growth factor and endothelin-1 on each gene expression. *Hypertension* 1998;32:89-95.
34. Gospodarowicz D. Biological activities of fibroblast growth factors. *Ann NY Acad Sci* 1986;638:1-8.
35. Gospodarowicz D, Ferrara N, Schweigerer L, et al. Structural characterization and biological functions of fibroblast growth factor. *Endocr Rev* 1987;8:95-114.
36. Mignatti P, Tsuboi R, Robbins E, et al. In vitro angiogenesis on the human amniotic membrane: requirement for basic fibroblast growth factor-induced proteinases. *J Cell Biol* 1989;108:671-82.
37. Yamamoto C, Kaji T, Furuya M, et al. Basic fibroblast growth factor suppresses tissue plasminogen activator release from cultured human umbilical vein endothelial cells but enhances that from cultured human aortic endothelial cells. *Thromb Res* 1994;73:255-63.
38. Le YJ, Corry PM. Hypoxia-induced bFGF gene expression is mediated through the JNK signal transduction pathway. *Mol Cell Biochem* 1999;202:1-8.
39. Koong AC, Denko NC, Hudson KM, et al. Candidate genes for the hypoxic tumor phenotype. *Cancer Res* 2000;60:883-7.
40. Miyazono K, Okabe T, Urabe A, et al. Purification and properties of an endothelial cell growth factor from human platelets. *J Biol Chem* 1987;262:4098-103.
41. Usuki K, Norberg L, Larsson E, et al. Localization of platelet-

- derived endothelial cell growth factor in human placenta and purification of an alternatively processed form. *Cell Regul* 1990; 1:577–84.
42. Ishikawa F, Miyazono K, Hellman U, et al. Identification of angiogenic activity and the cloning and expression of platelet-derived endothelial cell growth factor. *Nature* 1989;338:557–62.
 43. Martin L, Green B, Renshaw C, et al. Examining the technique of angiogenesis assessment in invasive breast cancer. *Br J Cancer* 1997;76:1046–54.
 44. Hettasch JM, Bandarenko N, Burchette JL, et al. Tissue transglutaminase expression in human breast cancer. *Lab Invest* 1996;75: 637–45.
 45. Heimann R, Ferguson D, Powers C, et al. Angiogenesis as a predictor of long-term survival for patients with node-negative breast cancer. *J Natl Cancer Inst* 1996;88:1764–9.
 46. Siltanen SM, Haapasalo HK, Rantala IS, et al. Comparison of different immunohistochemical methods in the assessment of angiogenesis: lack of prognostic value in a group of 77 selected node-negative breast carcinomas. *Mod Pathol* 1995;8:745–52.
 47. de Jong JS, van Diest PJ, Baak JP. Heterogeneity and reproducibility of microvessel counts in breast cancer. *Lab Invest* 1995;73: 922–6.
 48. Flug M, Kopf-Maier P. The basement membrane and its involvement in carcinoma cell invasion. *Acta Anat* 1995;152:69–84.
 49. Aho S, Rouda S, Kennedy SH, et al. Regulation of human interstitial collagenase (matrix metalloproteinase-1) promoter activity by fibroblast growth factor. *Eur J Biochem* 1997;247:503–10.
 50. Hoshi H, Konno S, Kikuchi M, et al. Fibroblast growth factor stimulates the gene expression and production of tissue inhibitor of metalloproteinase-1 in bovine granulosa cells. *In Vitro Cell Dev Biol Anim* 1995;31:559–63.
 51. Tsuboi R, Sato Y, Rifkin DB. Correlation of cell migration, cell invasion, receptor number, proteinase production, and basic fibroblast growth factor levels in endothelial cells. *J Cell Biol* 1990; 110:511–7.
 52. Götz C, Montenarh M. p53: DNA damage, DNA repair, and apoptosis. *Rev Physiol Biochem Pharmacol* 1996;127:65–95.
 53. Miller SD, Moses K, Jayaraman L, et al. Complex formation between p53 and replication protein A inhibits the sequence-specific DNA binding of p53 and is regulated by single-stranded DNA. *Mol Cell Biol* 1997;17:2194–201.
 54. Berardo M, Elledge RM, de Moor C, et al. Bcl-2 and apoptosis in lymph node positive breast carcinoma. *Cancer* 1998;82:1296–302.
 55. Evan GI, Wyllie AH, Gilbert CS, et al. Induction of apoptosis in fibroblasts by c-myc protein. *Cell* 1992;69:119–28.
 56. Keane MM, Ettenberg SA, Lowrey GA, et al. Fas expression and function in normal and malignant breast cell lines. *Cancer Res* 1996;56:4791–8.
 57. Sharma K, Srikant CB. Induction of wild-type p53, Bax, and acidic endonuclease during somatostatin-signaled apoptosis in MCF-7 human breast cancer cells. *Int J Cancer* 1998;76:259–66.
 58. Shiga A, Shirota K, Nomura Y. Immunohistochemical and ultrastructural studies on the sinusoidal lining cells of canine hepatocellular carcinoma. *J Vet Med Sci* 1996;58:909–14.
 59. Shiga A, Shirota K, Shida T, et al. Hepatoblastoma in a dog. *J Vet Med Sci* 1997;59:1167–70.
 60. Roy S, Sarkar C. Ultrastructural study of micro-blood vessels in human brain tumors and peritumoral tissue. *J Neurooncol* 1989;7: 283–92.
 61. Hirano A, Matsui T. Vascular structures in brain tumors. *Hum Pathol* 1975;6:611–21.
 62. Mendoza AS, Mentzel M, Krüger M, et al. The morphology of xenotransplanted human breast carcinoma MX1 growing in nude mice. A light and transmission electron microscopic study. *Ann Anat* 1995;177:3–10.
 63. Krüger M. Therapiebedingte Frühveränderungen der Zellkerne des MX1 Mammakarzinoms [Medical thesis]. Lübeck: Medical University of Lübeck, 1994.
 64. Stobbe EM. Effekte einer einmaligen Thermotherapie auf das menschliche, xenotransplantierte Mammakarzinom MX-1 [Medical thesis]. Lübeck: Medical University of Lübeck, 1997.
 65. Schmitt O, Eggers R, Krüger M, et al. Alterations of the nucleolar organiser regions (AgNORs) in the human MX1 xenograft after thermochemotherapy as detected by automatic image analysis. *J Anat* 1995;187:234–5.
 66. Mentzel M, Wiedemann G, Mendoza AS. The effect of ifosfamide on tumor oxygenation at different temperature. In: Vaupel P, ed. *Oxygen transport to tissue XV; Proceedings of the 20th ISOTT Conference held in Mainz, Germany*. New York: Plenum Press, 1994.
 67. Murrell TG. Epidemiological and biochemical support for a theory on the cause and prevention of breast cancer. *Med Hypotheses* 1991;36:389–96.
 68. Marxsen J, Schmitt O, Heits F, et al. Oxygen regulated VEGF gene expression in the human breast cancer cell line MX1 in vitro and in vivo. *Eur J Physiol* 1998;435:R128.
 69. Harmey JH, Dimitriadis E, Kay E, et al. Regulation of macrophage production of vascular endothelial growth factor (VEGF) by hypoxia and transforming growth factor beta-1. *Ann Surg Oncol* 1998;5:271–8.
 70. Harris AL, Zhang H, Moghaddam A, et al. Breast cancer angiogenesis—new approaches to therapy via antiangiogenesis, hypoxic activated drugs, and vascular targeting. *Breast Cancer Res Treat* 1996;38:97–108.
 71. Petit AM, Rak J, Hung MC, et al. Neutralizing antibodies against epidermal growth factor and ErbB-2/neu receptor tyrosine kinases down-regulate vascular endothelial growth factor production by tumor cells in vitro and in vivo: angiogenic implications for signal transduction therapy of solid tumors. *Am J Pathol* 1997;151:1523–30.
 72. Gospodarowicz D. Fibroblast growth factors: from genes to clinical applications. *Cell Biol Rev* 1991;25:307–16.
 73. Klein S, Giancotti FG, Presta M, et al. Basic fibroblast growth factor modulates integrin expression in microvascular endothelial cells. *Mol Biol Cell* 1993;4:973–82.
 74. Griffiths L, Dachs GU, Bicknell R, et al. The influence of oxygen tension and pH on the expression of platelet-derived endothelial cell growth factor/thymidine phosphorylase in human breast tumor cells grown in vitro and in vivo. *Cancer Res* 1997;57:570–2.
 75. Roberts WG, Pallade GE. Neovasculature induced by vascular endothelial growth factor is fenestrated. *Cancer Res* 1997;57:765–72.
 76. Esser S, Wolburg K, Wolburg H, et al. Vascular endothelial growth factor induces endothelial fenestrations in vitro. *J Cell Biol* 1998; 140:947–59.
 77. Khaw PT, Occleston NL, Schultz G, et al. Activation and suppression of fibroblast function. *Eye* 1994;8:188–95.
 78. Fukamizu H, Grinell F. Spatial organization of extracellular matrix and fibroblast activity: effects of serum, transforming growth factor beta, and fibronectin. *Exp Cell Res* 1990;190:276–82.
 79. Dyson JE, Simmons DM, Daniel J, et al. Kinetic and physical studies of cell death induced by chemotherapeutic agents or hyperthermia. *Cell Tissue Kinet* 1986;19:311–24.
 80. Allan DJ, Harmon BV. The morphologic categorization of cell death induced by mild hyperthermia and comparison with death induced by ionizing radiation and cytotoxic drugs. *Scan Electron Microsc* 1986;3:1121–33.
 81. Barry MA, Behnke CA, Eastman A. Activation of programmed cell death (apoptosis) by cisplatin, other anticancer drugs, toxins and hyperthermia. *Biochem Pharmacol* 1990;40:2353–62.
 82. Yao KS, Clayton M, O'Dwyer PJ. Apoptosis in human adenocarcinoma HT29 cells induced by exposure to hypoxia. *J Natl Cancer Inst* 1995;87:117–22.
 83. Joensuu H, Pylkkanen L, Tolkanen S. Bcl-2 protein expression and long-term survival in breast cancer. *Am J Pathol* 1994;145:1191–8.
 84. Debatin KM, Krammer PH. Resistance to APO-1 (CD95) induced apoptosis in T-ALL is determined by a BCL-2 independent anti-apoptotic program. *Leukemia* 1995;9:815–20.
 85. Teixeira C, Reed JC, Pratt MA. Estrogen promotes chemotherapeutic drug resistance by a mechanism involving Bcl-2 proto-oncogene expression in human breast cancer cells. *Cancer Res* 1995;55:3902–7.
 86. Szende B, Schally AV, Lapis K. Immunocytochemical demonstration of tissue transglutaminase indicative of programmed cell death (apoptosis) in hormone sensitive mammary tumours. *Acta Morphol Hung* 1991;39:53–8.